

number data and from about 500 body diameters for low Mach number data.

References

- Heckman, D., Tardif, L., and Lahaye, C., "Experimental Study of Turbulent Wakes in the CARDE Free-Flight Ranges," *Proceedings of the Symposium on Turbulence of Fluids and Plasmas*, Vol. XVIII, Polytechnic Press of the Polytechnic Institute of Brooklyn, N. Y., 1968.
- Lahaye, C., Leger, E. G., and Lemay, A., "Wake Velocity Measurements using a Sequence of Sparks," *AIAA Journal*, Vol. 5, No. 12, Dec. 1967, pp. 2274-2276.
- Heckman, D. et al., "A Shock Wave Attenuation Treatment for Ballistic Ranges," *AIAA Journal*, to be published.
- Herrmann, J., Slattery, R. E., and Clay, W. G., "Measured Properties of the Wakes of Hypersonic Cones," *AIAA Paper 68-687*, Los Angeles, Calif., 1968.
- Heckman, D., "Convection Velocity Measurements in Hypersonic Sphere Wakes," *AIAA Journal*, Vol. 6, No. 4, April 1968, pp. 750-752; also Heckman, D., private communication, 1969.
- Fox, J. and Rungaldier, H., "Anemometer Measurements of Velocity and Density in Projectile Wakes," *AIAA Paper 68-701*, Los Angeles, Calif., 1968.
- Ghosh, A. K. and Richard, C., "Probe Geometry Effect on Turbulent Plasma Diagnostics," Research Report 3.900.12, May 1968, R.C.A. Victor Company Ltd., Research Lab., Montreal.
- Lahaye, C., Leger, E. G., and Lemay, A., "Radial and Axial Velocity Profiles of Hypersonic and Supersonic Wakes Measured by the Sequential Spark Method," AGARD Conference Proceedings No. 19, Fluid Physics of Hypersonic Wakes Conference, May 1967.

Minimum-Time Attitude Maneuvers with Control Moment Gyroscopes

JACK KRANTON*

Bellcomm Inc., Washington, D. C.

A MANEUVER capability for large, Earth-orbiting space-craft such as a space station may be required to acquire new inertial attitudes for particular experiments and to manage the angular momentum accumulated by a CMG (control moment gyroscopes) system.¹

The solution to the maneuver problem with CMGs divides naturally into two parts, calculating the required control torque and commanding the CMG gimbal angle rates to produce that torque. Solutions to both problems are presented in this Note. These solutions can form the basis for implementation on flight hardware.

Rotation Angle and Rotation Axis

From Euler's rotation theorem,² it follows that any attitude maneuver can be expressed as a rotation through some angle (rotation angle) about some fixed axis (rotation axis). As in Ref. 3, \mathbf{e} will denote the unit rotation vector and Φ the rotation angle. Both \mathbf{e} and Φ are determined uniquely from the direction-cosine matrix between the coordinates that define the initial and final attitudes of the spacecraft.

During the maneuver \mathbf{e} is fixed relative to inertial coordinates and spacecraft coordinates, but the rotation angle $\phi(t)$ decreases to zero; that is, $\phi(0) = \Phi$ and $\phi(T) = 0$ where T is the total maneuver time. It is convenient to change variables and define the angle λ such that $\lambda(t) = \Phi - \phi(t)$, then $\lambda(0) = 0$ and $\lambda(T) = \Phi \equiv \Lambda$.

Received March 2, 1970; revision received May 4, 1970.

* Supervisor, Rotational Dynamics and Attitude Control Group, Apollo Applications Division. Member AIAA.

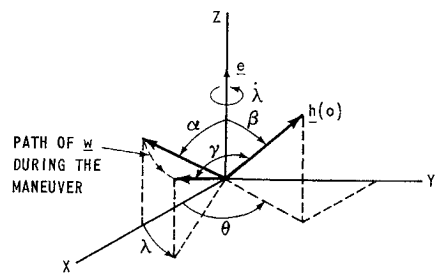


Fig. 1 Relationship between \mathbf{e} , $\mathbf{h}(0)$, and \mathbf{w} relative to inertial coordinates.

Control Torque for Minimum-Time Maneuver

The maneuver time will be minimum if at all times λ is maximized, subject to the constraint on the magnitude of the spin angular momentum vector \mathbf{H} of the CMG system. For a system of N CMGs each with a spin angular momentum of h , $|\mathbf{H}| \leq Nh$.

To determine the maximum λ , assume for the moment that the total angular momentum of the spacecraft and CMGs remains unchanged during the maneuver; that is, the effect of external torques is neglected during the maneuver. In vector-matrix notation, this can be stated as

$$\mathbf{H}(0) = \mathbf{H}(t) + I\omega = \mathbf{H}(t) + \lambda\mathbf{e} \quad (1)$$

where $\mathbf{H}(0)$ and $\mathbf{H}(t)$ are the total CMG spin angular momenta at times 0 and t , I is the inertia matrix, and $\omega (= \lambda\mathbf{e})$ is the angular velocity of the spacecraft. Note that $\mathbf{H}(0)$ and \mathbf{e} in Eq. (1) have a fixed orientation relative to inertial coordinates, but $\mathbf{H}(t)$ and $I\omega$ do not. It is convenient now to introduce the following notation: $\mathbf{H} = |\mathbf{H}|\mathbf{h} \equiv H\mathbf{h}$, $I\omega \equiv |I\mathbf{e}|\mathbf{w} \equiv W\mathbf{w}$ where \mathbf{h} and \mathbf{w} are unit vectors. With this notation, Eq. (1) can be rewritten as

$$H(t)\mathbf{h}(t) = -\lambda W\mathbf{w} + H(0)\mathbf{h}(0) \quad (2)$$

By forming the self dot product on both sides of Eq. (2), one obtains a quadratic equation for λ

$$H^2(t) = W^2\lambda^2 - 2H(0)Wc\gamma\lambda + H^2(0) \quad (3)$$

where $c\gamma = \mathbf{h}'(0)\mathbf{w}$ (sine and cosine are denoted by s and c). The maximum of λ is attained by choosing $H(t)$ to be the maximum Nh during the entire maneuver. Consequently, the maximum of λ is given by

$$\lambda = \{H(0)c\gamma + [-H^2(0)s^2\gamma + (Nh)^2]^{1/2}\}/W \equiv f(\lambda) \quad (4)$$

The functional relation between $c\gamma$ and λ can be determined by noting (see Fig. 1) that the vectors $\mathbf{h}(0)$ and \mathbf{e} are fixed, but \mathbf{w} rotates about \mathbf{e} with angular velocity λ . From the geometry, it follows that

$$c\gamma = \mathbf{h}'(0)\mathbf{w} = c\alpha c\beta + s\alpha s\beta c(\lambda - \theta) \quad (5)$$

where α , β , and θ are constant angles determined at the start of the maneuver from†

$$c\alpha = \mathbf{w}'\mathbf{e}, c\beta = \mathbf{h}'(0)\mathbf{e}, (0 \leq \alpha < \pi/2, 0 \leq \beta \leq \pi) \quad (6a)$$

and

$$\theta = \theta^+ \operatorname{sgn}[\mathbf{e}'[\tilde{\mathbf{w}}\mathbf{h}(0)]]|_{\lambda=0} \quad (6b)$$

where

$$\theta^+ = \cos^{-1}[(\mathbf{h}'(0)\mathbf{w} - c\alpha c\beta)/s\alpha s\beta]|_{\lambda=0} (0 \leq \theta^+ \leq \pi) \quad (6c)$$

Certain properties of $f(\lambda)$ are evident. The extreme values of $f(\lambda)$ coincide with the extreme values of $c\gamma$, which

† The symbol \sim over a vector indicates the cross product operation and the prime denotes transpose.

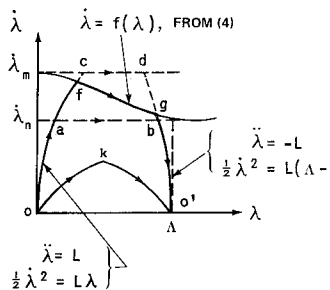


Fig. 2 Phase plane trajectories of maneuvers.

are $c(\alpha - \beta)$ and $c(\alpha + \beta)$. These extremes occur at $\lambda = \theta$ and $\lambda = \theta + \pi$; that is, when \mathbf{w} lies in the plane defined by \mathbf{e} and $\mathbf{h}(0)$. If α or β is zero, $f(\lambda)$ is constant for all λ . $\ddot{\lambda}$ is zero if the maneuver is about a principal axis of the spacecraft, for then \mathbf{e} and \mathbf{w} are colinear. β is zero if \mathbf{e} and $\mathbf{h}(0)$ are colinear. Also, if $H(0) = 0$, $f(\lambda)$ is constant for all λ and is equal to Nh/W .

The minimum-time maneuver is achieved by employing $\dot{\lambda} = f(\lambda)$ as given by Eq. (4). Such a maneuver is impossible to realize, for it would require that $\dot{\lambda}$ jump between zero and the values given by $f(\lambda)$ at the beginning and at the end of the maneuver. This no CMG system could achieve. To obtain a practical scheme, a bound must be placed on $\dot{\lambda}$; that is, $|\dot{\lambda}| \leq L$. With such a limit, the trajectory of a minimum-time maneuver in the phase plane has a shape ofgo' as shown in Fig. 2.

Bounds on the maneuver time T may be obtained readily. To do so, define $\dot{\lambda}_m$ and $\dot{\lambda}_n$ as the maximum and minimum values of $\dot{\lambda}$ as determined from $f(\lambda)$ for λ in the interval $[0, \Lambda]$; then

$$(\Lambda/\dot{\lambda}_m + \dot{\lambda}_m/L) < T < (\Lambda/\dot{\lambda}_n + \dot{\lambda}_n/L) \quad (7)$$

where the upper bound is obtained by following the trajectory oabo' on Fig. 2, and the lower bound by following the trajectory oedo'. It is advantageous to arrange matters such that $\theta = \Lambda/2$, for then $\dot{\lambda}_m$ would occur at $\lambda = \Lambda/2$, thereby lowering the maneuver time.

Trajectories such as ofgo' in Fig. 2 can be attained provided L is sufficiently large for the parabolic arcs to reach the curve defined by $\dot{\lambda} = f(\lambda)$. Maneuver trajectories such as o' would result for values of L that were not large enough.

The control torque \mathbf{T}_c required of the CMG system to produce spacecraft rotation about \mathbf{e} is determined by noting that $\dot{\omega} = \dot{\lambda}\mathbf{e}$ and $\dot{\omega} = \dot{\lambda}\mathbf{e}$; then

$$\mathbf{T}_c = -(\ddot{\lambda}\mathbf{I}\mathbf{e} + \dot{\lambda}^2\mathbf{e}\mathbf{I}\mathbf{e}) \quad (8)$$

The control torque here is taken as $\dot{\mathbf{H}}$, the total rate of change of spin angular momentum for the CMG system.

Effect of External Torques

In the preceding development the effect of external torques during the maneuver was neglected. To establish the effect, equate the external torque \mathbf{T}_{ext} to the rate of change of angular momentum

$$\mathbf{T}_{ext} = (d/d\tau)(I\dot{\omega} + \mathbf{H}) = (d/d\tau)(\dot{\lambda}\mathbf{I}\mathbf{e} + \mathbf{H}) \quad (9)$$

Integrating this equation, we get

$$H(t)\mathbf{h}(t) - \int_0^t \mathbf{T}_{ext} d\tau = -\dot{\lambda}W\mathbf{w} + H(0)\mathbf{h}(0) \quad (10)$$

Equation (10) is identical to Eq. (2) except for the term on the left involving the integral of the external torques. Thus the left side of Eq. (3) should be replaced by the square of the magnitude of the left side of Eq. (10). Then we can

\ddagger This is also true if β is π , but starting a maneuver with $\beta = \pi$ is undesirable.

write

$$\begin{aligned} |H(t)\mathbf{h}(t) - \int_0^t \mathbf{T}_{ext} d\tau|^2 &= |Nh(t) - \int_0^t \mathbf{T}_{ext} d\tau|^2 \\ &\geq (Nh - \max_{t(\leq T)} |\int_0^t \mathbf{T}_{ext} d\tau|)^2 \end{aligned} \quad (11)$$

where the $i(\leq T)$ connotes the worst case experience during the various maneuvers required of the spacecraft. A conservative value for the maximum $\dot{\lambda}$ is obtained, therefore, by replacing $(Nh)^2$ in Eq. (4) by the right side of the inequality in (11).

The effect of the external torques can also be taken into account in the calculation of the control torque; Eq. (8) becomes

$$\mathbf{T}_c = \mathbf{T}_{ext} - (\ddot{\lambda}\mathbf{e} + \dot{\lambda}^2\mathbf{e}\mathbf{I}\mathbf{e}) \quad (12)$$

Here it is presupposed that a mathematical model is used to calculate the external torques as a function of attitude and position in orbit.

These concepts form the basis of a practical, suboptimal scheme for executing maneuvers in near minimum-time.³

Commanded Gimbal Angle Rates for Arbitrary Control Torque

For any physical arrangement of CMGs on a spacecraft, the general expression for the control torque is

$$\mathbf{T}_c = \dot{\mathbf{H}} = h[G\dot{\alpha} + F\dot{\beta} + \omega\mathbf{h}^t] \quad (13)$$

where h = magnitude of spin angular momentum for each CMG; $G, F = 3 \times N$ matrices of gimbal angles (N two-degree-of-freedom CMGs are assumed); $\dot{\alpha}, \dot{\beta} = N \times 1$ column vectors of outer and inner gimbal angle rates, respectively; $\omega\mathbf{h}^t$ = cross product of the spacecraft angular velocity and the per unit total spin angular momentum of the system (i.e., $\mathbf{H} = h\mathbf{h}^t$).

Any solution for $\dot{\alpha}$ and $\dot{\beta}$ that satisfies Eq. (13) is all that is required to produce \mathbf{T}_c exactly. A direct solution for $\dot{\alpha}$ and $\dot{\beta}$ cannot be obtained from Eq. (13) because there are $2N$ unknowns in 3 equations. A straightforward approach to this problem is to introduce an objective function in $\dot{\alpha}$ and $\dot{\beta}$ that we wish to minimize and treat Eq. (13) as a set of constraint equations. The objective function chosen is

$$\dot{J} = \frac{1}{2}(\dot{\alpha}^2 + g\dot{\beta}^2) \quad (14)$$

which reflects an interest in minimizing the dynamic range of the gimbal angle rates.

This minimization problem can be solved by the method of Lagrange multipliers. The solution is

$$\begin{aligned} \dot{\alpha} &= G'[GG' + (1/g)FF']^{-1}[(1/h)\mathbf{T}_c - \omega\mathbf{h}^t] \\ &= (1/g)F'[GG' + (1/g)FF']^{-1}[(1/h)\mathbf{T}_c - \omega\mathbf{h}^t] \end{aligned} \quad (15)$$

The scalar g is positive and is chosen by the system designer to equalize, if possible, the dynamic range of the inner and outer gimbal rates as observed in simulations of system response to worst case control situations.

The preceding solution for $\dot{\alpha}$ and $\dot{\beta}$ requires that the matrix $(GG' + (1/g)FF')$ be of rank 3. Physically this means that for an arbitrary vector $[(1/h)\mathbf{T}_c - \omega\mathbf{h}^t]$ there is some $\dot{\alpha}, \dot{\beta}$ that solves Eq. (13). But this requirement would exist for any procedure that attempts to solve Eq. (13). Hence, the solution has introduced no special restrictions on system performance.

References

¹ Koenig, H. F., "Angular Momentum Desaturation for ATM/LM/CSM Configuration using Gravity Gradient Torques," TMX-53764, Aug. 1968, NASA.
² Goldstein, H., *Classical Mechanics*, Addison-Wesley, Reading, Mass., 1950, p. 118.
³ Kranton, J., "Application of Optimal Control Theory to Attitude Control with Control Moment Gyroscopes," D.Sc. dissertation, Feb. 1970, George Washington Univ., Washington, D.C.

Laminar Viscous Effects over Blunt Cones at Hypersonic Conditions

CLARK H. LEWIS*

Virginia Polytechnic Institute, Blacksburg, Va.

Nomenclature

C_{Df} = friction-drag coefficient referenced to base area
 M = Mach number
 r_b, r_n = base and nose radii, respectively
 U_∞ = freestream velocity
 ϵ = $(\mu^*(U_\infty^{*2}/C_p^*)/\rho_\infty^* U_\infty^* r_n^*)^{1/2}$, Van Dyke's expansion parameter

Subscripts

0 = stagnation conditions
 STJ = slip and temperature jump effect
 TVC = transverse curvature effect
 vort = vorticity effect
 w = wall
 $*$ = dimensional quantity

SPHERICALLY blunted cones have been used extensively in experimental studies at supersonic and hypersonic conditions. Since classical laminar boundary-layer theory has not been successful under moderately low Reynolds number conditions, a need has existed for several years for a theoretical model to explain the experimental observations such as pressure and heat-transfer distributions over bodies and prediction of zero-lift drag. It turns out that the skin-friction drag is more sensitive to low Reynolds number viscous effects than are the pressure and heat-transfer distributions. Also the prediction of zero-lift drag is important in the analysis of wind-tunnel data.

Theoretical analysis of viscous effects at hypersonic conditions can proceed in either of two ways. Early extensions of classical boundary-layer theory considered the effects of longitudinal body curvature (LC). More recently the separate effects of transverse curvature (TVC), and slip and temperature jump (STJ) were considered. The last effect to receive attention was shock generated external vorticity (vort) in the stagnation region of blunt bodies. These effects are considered by including the next order of terms in the boundary-layer equations (LC and TVC) and by modifying the wall and outer edge boundary conditions (STJ and vort). The remaining effect of the same order of magnitude but not mentioned previously is boundary-layer displacement effect (disp) which is a global effect and must be considered with the entire external inviscid flowfield. The approach described

previously is called herein a first-order treatment of higher-order boundary-layer effects.

Another treatment of higher-order effects is based upon a perturbation expansion of the variables in the Navier-Stokes equations and the method of matched asymptotic expansions. Retaining first-order terms gives the classical Prandtl boundary-layer equations. Second-order terms include all the effects described in first-order treatment.

The primary difference between the first- and second-order treatments of higher-order effects is that the higher-order effects in second-order theory are with one exception linearly independent whereas the effects in the first-order treatment are coupled, nonlinear effects. It is therefore of interest to consider comparison of the two theories with each other as well as comparison of each with experimental data.

Experimental data from wind-tunnel tests have provided the incentive for a study of higher-order boundary-layer effects under nearly perfect gas conditions. Several years ago the strong influence of higher-order viscous effects was experimentally observed on the drag of slender cones at $M_\infty = 10$ to 20.¹ Since that time a study of theoretical and numerical methods has been made to analyze and predict observed experimental trends. To date the best available theoretical models and numerical methods have not been successful in predicting the observed results over the entire ranges of Mach and Reynolds numbers experimentally studied.

The purpose of the present paper is to indicate the results of the application of first- and second-order boundary-layer theories to a sphere-cone for a range of Reynolds numbers at $M_\infty = 18$, and comparisons with experimental data indicate where one might expect the theoretical models to be applicable.

Lewis and Whitfield¹ presented some of the early work done in von Karman Gas Dynamics Facility (VKF) where they applied iterated inviscid-viscous flowfields models to predict pressure and heat-transfer distributions and zero-lift drag of a 9° half-angle, spherically blunted cone at $M_\infty = 18$. In that work an inverse blunt body and characteristics solution for the inviscid outer flow was iterated with a first-order boundary-layer solution which included approximate transverse curvature terms. The blunt body and characteristics method used was due to Inouye, Rakich, and Lomax² and the boundary-layer method was that of Clutter and Smith.³ In many respects the results of the predictions of Lewis and Whitfield were in surprisingly good agreement with the experimental results since the effects of shock-generated external vorticity and slip and temperature jump were not considered and the effects of transverse curvature and displacement were only approximately treated.

Davis and Flügge-Lotz⁴ considered second-order boundary-layer effects on hyperboloids, paraboloids, and spheres at infinite Mach number and ten, respectively. The theory of Van Dyke⁵ was used with an implicit finite-difference scheme originally proposed by Flügge-Lotz and Blottner⁶ for treating the classical first-order boundary-layer equations for two-dimensional flows. As will be shown in this paper, the theory of Van Dyke when coupled with the implicit finite-difference method of Davis and Flügge-Lotz gives a powerful tool for extending classical boundary-layer theory to lower Reynolds number.

In addition to the second-order treatment based on Van Dyke-Davis and Flügge-Lotz, a first-order treatment of vorticity, displacement, transverse curvature (TVC), and slip and temperature jump (STJ) was developed by the author⁷ based on a modification of the first-order boundary-layer method of Clutter and Smith. The treatment of vorticity is based on the suggestion of Hayes and Probstein⁸ where the outer boundary condition is changed to account for an increase in velocity and a nonzero velocity gradient.

Second-order boundary-layer theory is discussed in Refs. 7 and 9-12. The numerical methods used to compute the

Received December 30, 1969; revision received April 20, 1970. This work was partially supported by the Arnold Engineering Development Center under contract F40600-69-C-0001 with ARO, Inc. The author acknowledges the assistance of J. C. Adams and E. O. Marchand who furnished the second-order boundary-layer solutions.

* Professor of Aerospace Engineering. Associate Fellow AIAA.